

RSC Advances



This is an *Accepted Manuscript*, which has been through the Royal Society of Chemistry peer review process and has been accepted for publication.

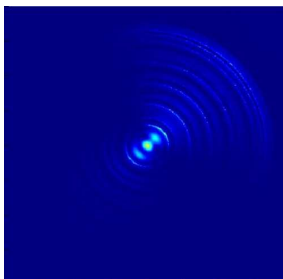
Accepted Manuscripts are published online shortly after acceptance, before technical editing, formatting and proof reading. Using this free service, authors can make their results available to the community, in citable form, before we publish the edited article. This *Accepted Manuscript* will be replaced by the edited, formatted and paginated article as soon as this is available.

You can find more information about *Accepted Manuscripts* in the [Information for Authors](#).

Please note that technical editing may introduce minor changes to the text and/or graphics, which may alter content. The journal's standard [Terms & Conditions](#) and the [Ethical guidelines](#) still apply. In no event shall the Royal Society of Chemistry be held responsible for any errors or omissions in this *Accepted Manuscript* or any consequences arising from the use of any information it contains.

A table of Contents Entry

* Colour Graphic



*Text

We show the manipulation of the overall polarization orientation of the enhanced and confined surface Plasmon polaritons near the nanostructure.

Controlling the polarization orientation of highly confined and enhanced surface plasmon polaritons

Dawei Zhang,^{1,2} Mengjun Zhu,¹ Linwei Zhu,² Qinfeng Xu³ and Jiannong Chen,^{2,*}

¹Engineering Research Center of Optical Instrument and System, Ministry of Education, Shanghai Key Lab of Modern Optical System, School of Optical-Electrical and Computer Engineering, University of Shanghai for Science and Technology, 516 Jungong Rd, Shanghai 200093, China

²School of Physics and Optical-Electrical Engineering, Ludong University, Yantai 264025, China

³School of physics, Nanjing University, Nanjing, China

*13220935107@163.com

We demonstrate a schematic method to tune and control the polarization orientation of surface Plasmon polaritons highly confined and enhanced to nanoscale spot. The two types of nanostructures are used and illuminated with specially designed excitation source which is created by directing a radially polarized beam onto a half-blocked linear polarizer. The overall polarization orientation is defined and calculated. It is demonstrated that the azimuthal angle of the overall polarization orientation can be arbitrarily tuned by rotating the one lobe linearly polarized beam azimuthally and the polar angle of the overall polarization orientation can be adjusted by using the different thick circular disk with the diameter less than the wavelength of the surface plasmon polaritons. The highly confined and enhanced light field with tunable polarization orientation may make many applications more attractive and applicable, especially for polarization-sensitive sensing technique and other nanoscale device.

1. Introduction

Surface plasmon polaritons (SPPs) are the collective oscillations of free electrons at metal and dielectric interfaces excited by external illumination. The SPPs offers a route to control light fields with metallic nanostructures. These nanostructures can tightly confine electromagnetic energy into nanoscale volume and accordingly enhanced the light field compared with the incident light field. These properties have enabled breakthroughs in diverse applications including super-resolution Imaging,^{1,2} single-molecule detection,³ surface enhanced Raman scattering (SERS),⁴ biological sensing,⁵ photovoltaics,⁶ quantum communications,^{7,8} nanocircuitry,^{9,10} and metamaterials.^{11,12} Thus the nanostructures and manipulation of SPPs is currently an attractive research subject. Up to date, various nanostructures and illumination schemes for confining, enhancing and manipulating the SPPs have been proposed.¹³⁻²⁷

In the far field sub-wavelength focusing of objectives, the modulation of amplitude, phase and polarization of incident beams for manipulating the shape and polarization of subwavelength focusing spot has been intensively investigated.²⁸⁻³⁸ However, the polarization manipulation of the surface Plasmon polaritons in the near field of nanostructures is seldom reported. It seems that the SPPs always propagate along the metal surface resulting in the dominant out-of-plane component

of the polarization. However, in the confined and enhanced nanoscale spot, the superposition and interference of SPPs originated from various directions and different parts of the nanostructure should change the overall polarization orientation. The asymmetry of the nanostructure, the anisotropic property of materials and the varied illumination sources with different polarization state and intensity distribution will also result in the different orientations of overall polarization in nanoscale electric field. On the other hand, when we probe into the field around more small nanostructure such as the tip, hole, slit or the corner of the metal materials,^{16,18,19,39} the vector orientation of the electric field is not simply an out-of-plane component. It is obvious that the polarization state in the near field of the nanostructure also strongly depends on the local geometrical shape of the metal. Conversely, the polarization state in the confined field contains the information of the incident beam and the nanostructure.

In this paper, motivated by applications such as probe of near-field imaging,⁴⁰⁻⁴² polarization-sensitive fluorescence emission rate,³⁸ plasmonic lithography,⁴³ we proposed two nanostructures illuminated with radially polarized beam filtered by a half-blocked linear polarizer for manipulating the polarization state of the confined and enhanced light field. The first nanostructure is made of several periodic annular slits milled into the thin layer of gold film with a small gold disk located in the center; the second nanostructure is composed of circularly arranged and equally spaced multiple pairs of specially designed two rectangle slits. We calculated the confined and enhanced nanoscale surface plasmonic field located at the center of the nanostructure when it is illuminated by a radially polarized beam along with a half-blocked rotatable linear polarizer. We also defined and calculated the overall polarization orientation composed of the azimuthal angle with respect to the x-axis and the polar angle with respect to the z-axis. It is found that the overall polarization orientation can be tuned azimuthally. The polar angle of the polarization with respect to z-axis is also controllable by adjusting the thickness of the circular disk in the center of the nanostructure.

2. The nanostructure and the excitation field

We describe the first nanostructure for confining and enhancing the electric field. It is a surface plasmonic lens (SPL). Fig.1 illustrates the entire nanostructure. Fig.1 (a) is the perspective view of the nanostructure with the inset being the close-up of the central part. Fig.1 (b) is the side view crossing the center of the nanostructure. The concentric periodic annular slits milled into the gold film and titanium film with thickness of 120nm and 30nm, respectively, are designed for exciting propagating surface plasmon polaritons. The widths of the slits are around 200nm. The period of the annular slits is equal to the wavelength of surface plasmonic wave. When the wavelength of external excitation laser is 633nm, the respective wavelength of surface plasmonic polaritons is around 600nm. The outmost annular slit is a half of the period away from the adjacent annular slit for reflecting the outward propagating SPPs into inward propagating SPPs. For the concentric periodic annular slits, the best excitation source is the radially polarized beam. The SPPs propagates along the interface between the metal and dielectric medium with the electric field component dominantly perpendicular to the surface. As a result of interfering constructively, a focusing nanoscale spot with the size of half wavelength is created in the center of this concentric circular periodic annular slits. The electric field component in focusing spot may change the spatial orientation when encountering any of nanoscale grooves, pits, holes, tips, disks or corners. In the near field of such special physical structure, the surface plasmonic polaritons is also affected by the way of the illumination. The overall polarization in a small volume mainly

depends on the strong and dominant local polarization component. To increase the degree of freedom in tuning the polarization, a circular disk is positioned in the center of the nanostructure. Accordingly, the focusing electric field will further excite the localized surface plasmon on the small, and circular gold disk, generating confined and enhanced nanoscale electric field with more freedom of tuning polarization.

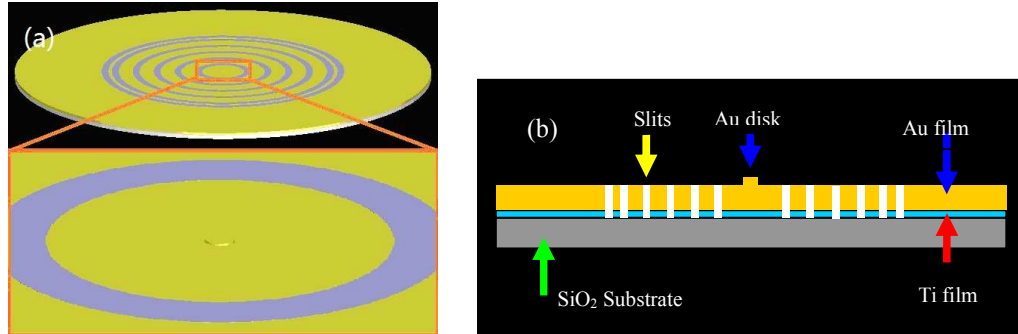


Fig.1. The first nanostructure for confining and enhancing the surface plasmon polaritons which can be excited by the radially polarized beam. The incident beam is directed onto the nanostructure from the side of the substrate. (a) The perspective view and the close-up of the central part; (b) the side view of the nanostructure.

The second nanostructure for confining and enhancing the electric field is shown in the Fig.2. Here it is termed as the structure for all-type polarization illumination (shortened as SATPI). The gold film and titanium film with thickness of 120nm and 30nm are deposited on the SiO₂ substrate. The ring-shaped multiple pairs of two mutually perpendicular rectangular slits can be fabricated by the focused ion beam (FIB). The each single pair of rectangular slits is specially designed as shown in Fig. 2(a). The center of the blue dashed rectangle is located at the origin of XY coordinates system. The two gray rectangles denote two slits milled into the gold film. The green line oriented along with the radial direction of the overall nanostructure as shown in Fig. 2(b) passes through the origin of the coordinate system as illustrated in the Fig. 2(a). The parameters are as follows:⁴² $W = 40nm$, $L = 200nm$, $M = 90nm$, $N = 120nm$. The radius R of the red circle is around $3000nm$. The number of the total pairs on the annular circle is 90. The spacing distance between two adjacent pairs is around 210nm. With these structure parameters, the λ_{SPP} on the interface between gold and air are larger than the length of the narrow aperture.

For SPPs excitation, usually only the component of the incident light that is polarized perpendicularly to the slits can be coupled into SPPs, leading to a decrease in the SPP signal and a loss of information about the incident polarization state.³⁸ However, for a narrow rectangular subwavelength slits, the SPP emission pattern is approximately that of an in-plane dipole.⁴⁵ A pair of such two mutually perpendicular rectangular subwavelength slits both of which are oriented 45° with respect to the radial direction can be excited by incident linear polarized beam, radially polarized beam and circularly polarized beam. When multiple pairs of such two slits are arranged in an annular shape with spacing between two adjacent pairs less than the λ_{SPP} , the launched SPPs can be viewed as converging plane waves.⁴² This effect is independent of the orientation of the individual narrow aperture. Thus the nanostructures are not sensitive to the polarization orientation in excitation. In the following section, we show that both of the circularly polarized

incident illumination and radially polarized incident illumination can excite the SPPs propagating towards the center of the nanostructure.

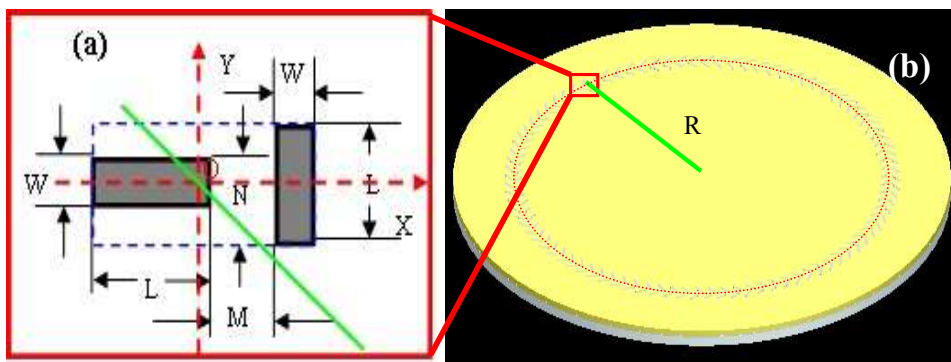
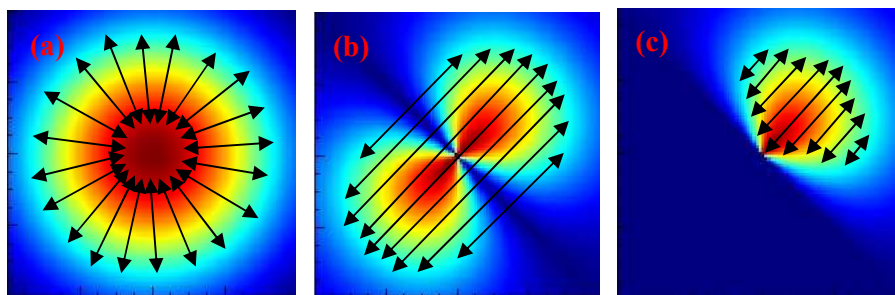


Fig.2 The second nanostructure for confining and enhancing the surface plasmon polaritons which can be excited by both of the radially polarized beam and circularly polarized beam. (a) A single pair of two rectangular slits; (b) the overall structure composed of 90 pairs of two rectangular slits arranged on the circle with the radius of 3000nm. The red dotted circular line is not structure, it is only for denoting the radius.

Both of two nanostructures described above are capable of confining and enhancing the electric field to a nanoscale spot in the center of the nanostructure. To realize the tuning of the polarization state in the confined and enhanced nanoscale spot, we designed a linearly polarized one lobe illumination source which can be rotated azimuthally. It is obtained as follows: first, a radially polarized Gaussian beam as shown in Fig. 3(a) is filtered by a linear polarizer. It becomes a linearly polarized two lobe illumination source as illustrated in Fig. 3(b). Second, the one lobe of the linearly polarized two lobe illumination source is completely blocked. It is shown in the Fig.3(c). The detailed descriptions of the polarization and intensity transformation are given in the supplementary information. For comparison, Figure 3(d) shows a cross-section intensity distribution of a linearly polarized Gaussian beam. When half of it is blocked, it becomes a linearly polarized half beam as illustrated in Fig. 3(e). There is the difference between Fig. 3(c) and Fig. 3(e) in intensity distribution. Obviously, Fig. 3(c) should be a better choice for azimuthally controllable illumination. The above-mentioned two nanostructures are both circularly symmetrical. When they are illuminated by using the light source as described in Fig. 3(c), the azimuthal angle of the overall polarization of highly enhanced and confined nanoscale spot in the center of the nanostructure is expected to be tunable.



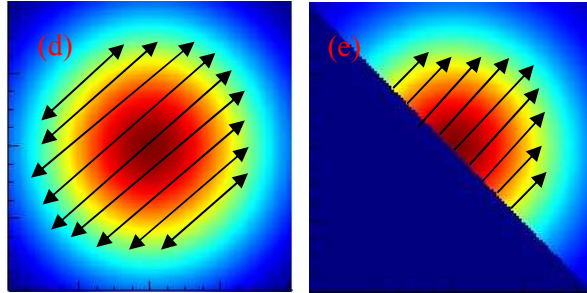


Fig.3 the illumination source for tuning the polarization of the enhanced electric field nanoscale spot confined in the near field of the nanostructures. (a) a radially polarized Gaussian beam; (b) a linearly polarized two-lobe beam which is created by passing the radially polarized beam through an aligned linear polarizer which can be rotated; (c) a linearly polarized one-lobe beam created by passing the radially polarized Gaussian beam through a half-blocked linear polarizer; (d) a linearly polarized Gaussian beam; (e) a half-blocked linearly polarized Gaussian beam

3. The enhancement and confinement of the SPPs

We use commercial FDTD Solutions to calculate the electric field distribution in the near field of the nanostructures described in section 2. The first nanostructure (SPL) as illustrated in the Fig.1 is designed for illumination wavelength of 633nm. With the illumination of radially polarized beam, the SPP intensity distribution on the monitor normal to the z axis which is 10nm away from the gold film surface is shown in the Fig.4. Figure 4(a) is the total intensity distribution. The intensity enhancement factor compared to the maximum incident intensity is as high as 240. The FWHM (full width at half maximum) is around 200nm. Figure 4(b) is the close-up of the central part in Fig. 4(a). Figure 4(c), Figure 4(d) and Figure 4(e) are the intensity distributions of three electrical field components E_x , E_y and E_z , respectively. It is seen that the central nanoscale spot is mainly composed of E_z component which is polarized perpendicular to the metal surface.

The second nanostructure (SATPI) with the parameters described in section 2 and illustrated in Fig.2 is also designed for excitation wavelength of 633nm. To verify the feasibility of the structure parameters, we use different wavelengths in both of circularly polarized beams and radially polarized beams to calculate the intensity distribution of the SPPs in the near field of the gold film. In this calculation, a circular gold disk with thickness of 10nm and diameter of 100nm is placed at the center of this nanostructure. Fig.5 shows the wavelength dependence of the enhancement factors. It is found that the wavelength of 633nm in both of circularly polarized beam illumination and radially polarized beam illumination are optimized value for maximum enhancement. It is also obvious that the enhancement of the confined nanoscale electric field spot obtained by circularly polarized beam illumination is better than that of the confined nanoscale electric field spot obtained by radially polarized beam illumination. This performance can be attributed to the unidirectional propagation property of the second nanostructure when it is a vertical line column and illuminated with circularly polarized beam.⁴² The theoretical explanation and graphical illustration (see Fig.S3 and Fig.S4) can be found in supplementary information. If we define the bandwidth as the wavelength range in which the enhancement is larger than half of the maximum enhancement, the bandwidth of this nanostructure is roughly 220nm both for circularly polarized beams and radially polarized beams illumination. It is limited to the visible

illumination with the center wavelength of 633nm.

One of the most attractive applications of the highly enhanced and confined nanoscale electrical field is the excitation and imaging of Raman spectrum. With the nanostructures described above, the enhanced and confined electrical field is located at the center of the nanostructure. When a cone-shaped gold nanoparticle is fabricated at the center, the more strong localized surface plasmons will be further excited at the tip of this cone-shaped nanoparticle. This nanoparticle with sharp tip could serve as a probe for scanning the sample and imaging the Raman spectrum (usually it is termed tip-enhanced Raman spectroscopy). We calculated tip enhancement for the first nanostructure with a cone-shaped gold nanoparticle at the center when it is illuminated with the radially polarized beam. The diameter of cone base is 100nm and the height of it is 300nm. The calculation shows that the intensity enhancement factors could be six orders higher than that of the incoming illumination light (Fig.S5).

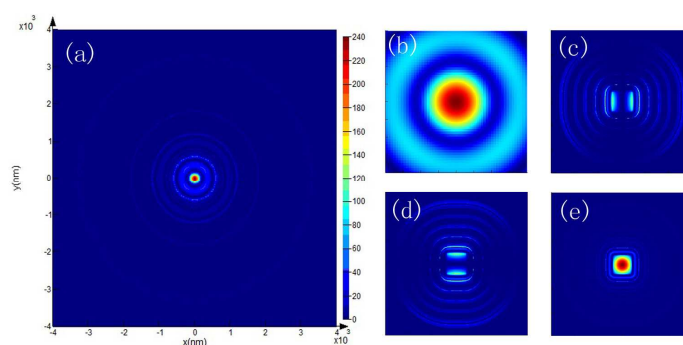


Fig.4 The intensity distribution of SPPs when the first nanostructure shown in Fig.1 is illuminated with the radially polarized beam. The size of the monitor is 8000nm \times 8000nm. The monitor parallel to the surface of the gold film is 10nm away from the surface.

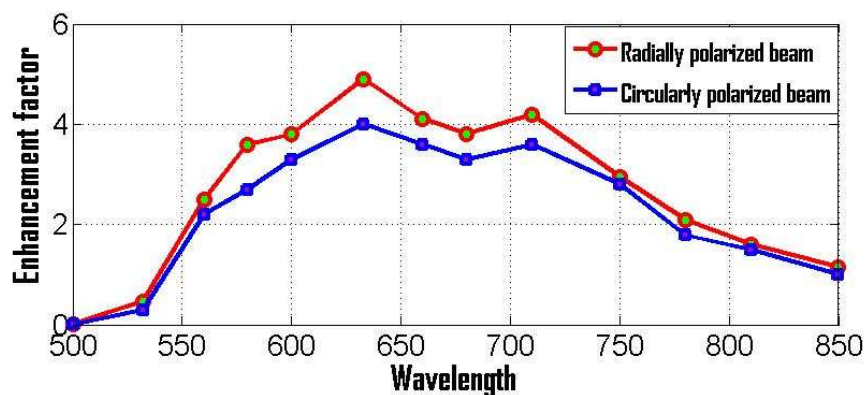


Fig.5 The enhancement dependence on the illumination wavelengths when the second nanostructure (SATPI) is illuminated.

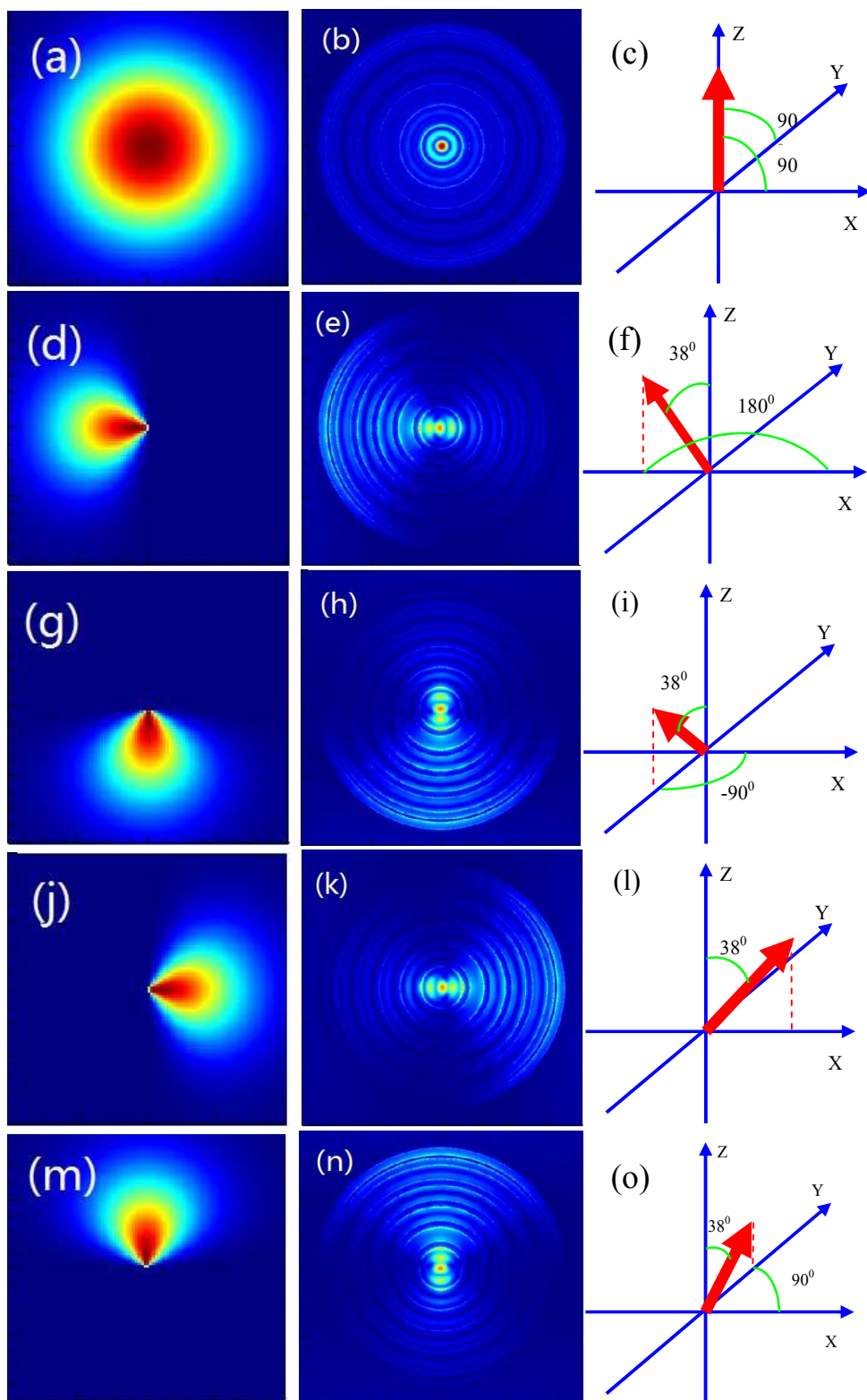
4. The characterization and manipulation of the polarization in the nanoscale spot

In this section, we propose a conception of the overall polarization effect of three-dimensional confined and enhanced nanoscale electric field spot. Then we demonstrate a scheme for tuning the polarization azimuthally and the polarization polar angle with respect to the z-axis.

In Ref.(38), an arbitrary polarization manipulation is achieved in a subwavelength focal plane of the high numerical aperture objective by directing differently weighed radially polarized beam and azimuthally polarized beam simultaneously onto the azimuthally apodized back aperture of the objective. However, the strongest light intensity is not necessary located on the focal plane. The light field out of the focal plane will certainly interact with the matters such as relatively big nanorods or small dipolar molecule. In our investigation, we consider characterization and manipulation of the overall polarization effect in a nanoscale volume near the metal surface of the nanostructure. To describe the overall polarization effect on the polarization-sensitive matters, we assume that there is a cubic box encompassing the enhanced and confined nanoscale spot which was divided into $M \times M \times N$ unit cells. In each unit cell, the magnitude and the direction of the electric field vector is assumed to be a constant. Considering phase difference among the unit cells, we defined and calculated the three electric field components, the azimuthal angle and the polar angle of the overall polarization orientation as shown in Fig.S6. The detailed definition and calculation formulae can be found in supplementary information.

4.1 The SPL with linearly polarized one-lobe illumination

We first choose illuminating the SPL with no disk at the center in six way: all-around, left side, bottom, right side, top and tilted as shown in the Fig.6(a), (d), (g), (j), (m) and (p). Fig.6 (b), (e), (h), (k), (n) and (q) are the respective intensity distribution. The red arrow in Fig.6 (c), (f), (i), (l), (o) and (r) are the respective overall polarization orientation described by azimuthal angle and polar angle with respect to the z-axis. It is obvious that the azimuthal angles change along with the illumination way. By rotating the half-blocked linear polarizer, the polarization orientation of the confined and enhanced nanoscale electric field will change azimuthally. However, the polar angle with respect to the z-axis remains almost the same. We expect that the polar angle depends on the intensity distribution of the one lobe linear polarized beam. For this reason, the FWHM (full width at half maximum) of the radially polarized beam has been increased from 12000nm to 16000nm. We calculated the intensity distribution and polarization orientation in the case of left side illumination. The result is demonstrated in Fig.6(s), (t) and (u). It is found that the polar angle depends on the intensity distribution of the illumination of the nanostructure. Another approach to tune the polar angle is to put a circular disk with the diameter less than the λ_{SPP} . By changing the thickness, the polar angle of the overall polarization will change drastically. It is illustrated in Fig.7. Fig.7 (a), (b), (c) and (d) are the intensity distributions and polarization states for the circular disk with thickness of 10nm; Fig.7 (e), (f), (g) and (h) are the intensity distributions and polarization states for the circular disk with thickness of 20nm; It is demonstrated that the polar angle of the overall polarization strongly depends on the thickness of the circular disk in the center of the nanostructure. The intensity distribution is also influenced. It should be noted that, in order to tune the polarization orientation, the disk diameter has to be much less than the wavelength of the SPPs since the size of the confined electric field is less than the wavelength of the SPPs. In this investigation, the diameter of the disk is set to be 100nm. How this parameter is determined are given in supplementary information.



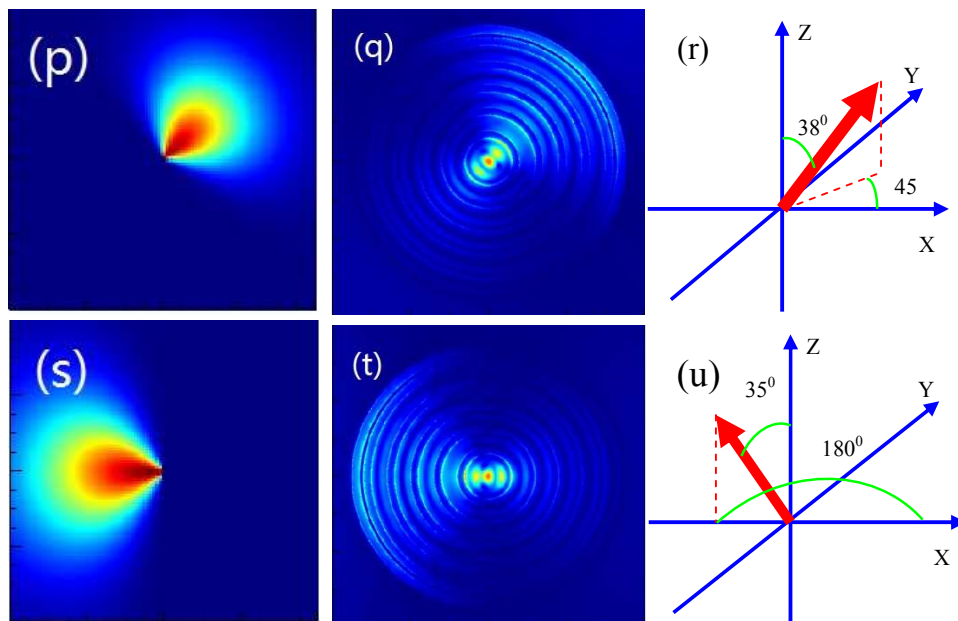
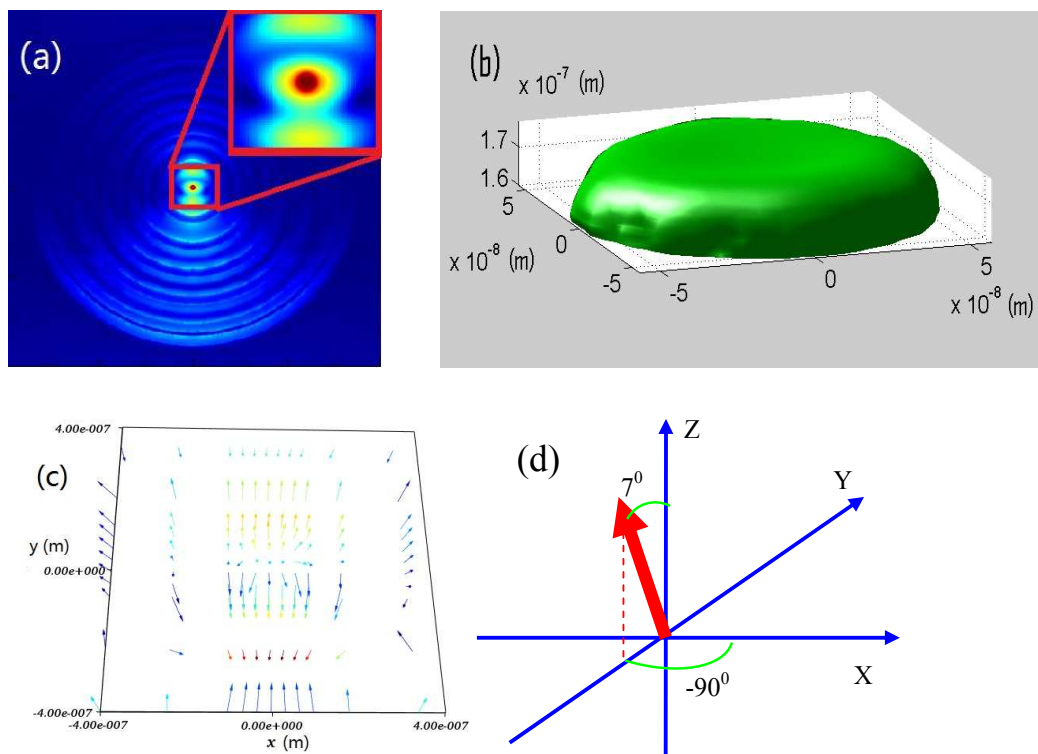


Fig.6 The illumination way, the intensity distribution in the near field of the nanostructure and the respective overall polarization orientation of the confined and enhanced nanoscale volume. In (a), (d), (g), (j), (m) and (p), the intensity distribution of the cross-section of the radially polarized beam before passing through the half-blocked linear polarizer has the FWHM of 12000nm. In (s), the FWHMs are 16000nm. The polar angles of the overall orientation are 35° .



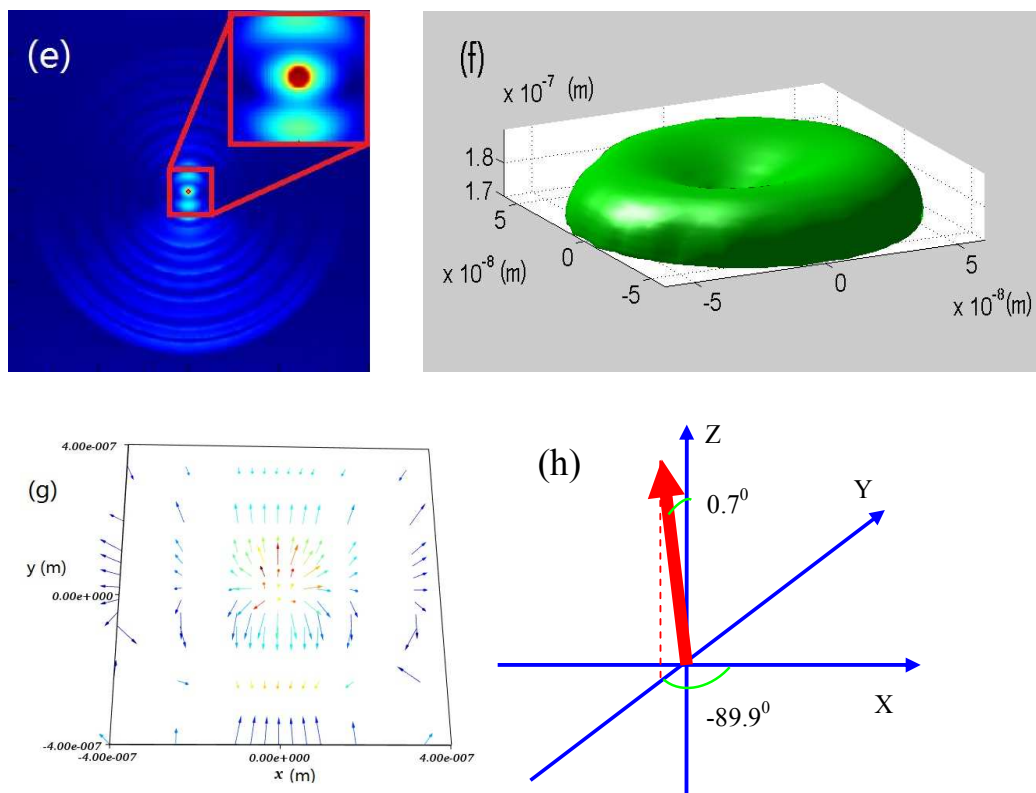


Fig.7 The polar angle of the overall polarization can be tuned when a small circular disk with the diameter less than the wavelength of the SPP is present at the center of the SPL. In Fig.7 (a) , (b),(c) and (d), the thickness of the disk is 10nm and polar angle is 7° . In Fig.7 (e),(f), (g) and (h), the thickness of the disk is 20nm and polar angle is 0.7° . The diameters in both of cases are 100nm.

4.2 The SATPI with linearly polarized one-lobe illumination

The circularly polarized beam is constructed with two linearly polarized beams. The polarization orientations of two linearly polarized beams are perpendicular to each other and there exist a phase difference of $\pi/2$. The investigation and calculation shows that, when a circularly polarized beam illuminates only a segment of SATPI nanostructure, the polarization orientation of the confined and enhanced nanoscale is not azimuthally adjustable as expected. To tune the polarization orientation, we still use the linearly polarized one-lobe beam to illuminate the arc-shaped segment of SATPI nanostructure as illustrated in Fig.8. As verified in Fig.9, the azimuthal angle of the overall polarization in a nanoscale volume located at the center of the arc-shaped nanostructure is expectedly adjustable.

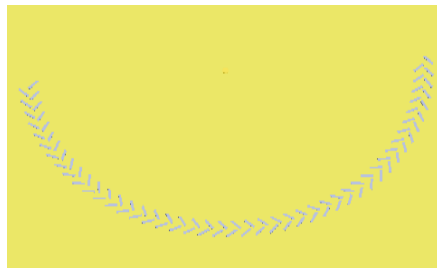


Fig.8 an arc-shaped segment of SATPI

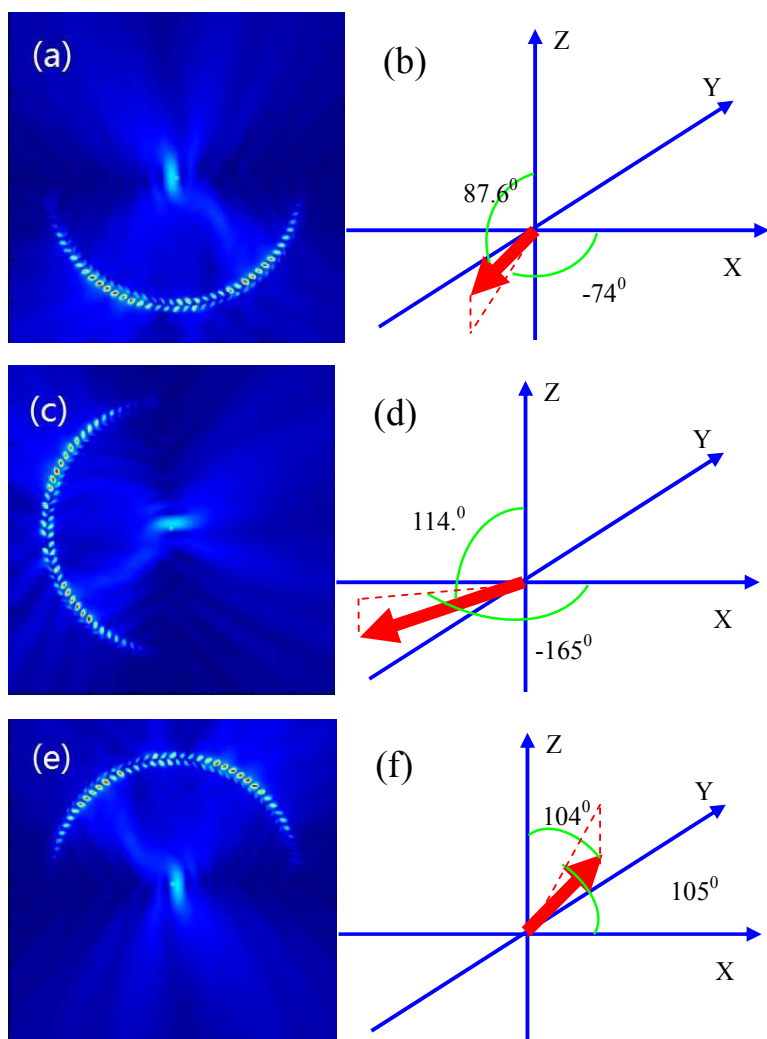


Fig.9 tuning the polarization orientation of the nanoscale electric field volume created at the center of the arc-shaped and segmented SATPI when it is illuminated with an azimuthally adjustable and linearly polarized one lobe beam

5. Summary

We have demonstrated that the polarization orientation of the confined and enhanced surface plasmon polaritons in a nanoscale volume can be controlled and tuned in terms of both of azimuthal angle and polar angle with respect to z-axis by using azimuthally adjustable and linearly polarized one lobe illumination sources. We show that, two nanostructures, the surface plasmonic lens (SPL) composed of a series of periodic annular slits milled into the gold film with a circular disk and the structure for all-type polarization illumination (shortened as SATPI) can be used to tune the overall polarization orientation. The azimuthally adjustable and linearly polarized one lobe illumination sources can be created by directing a radially polarized beam onto an aligned and half-blocked linear polarizer. The tunable nature of overall polarization orientation of a confined and enhanced nanoscale electric field may open up the possibility of many nanoscale polarization-sensitive applications and opto-electric devices.

Acknowledgement

This work is supported by the National Natural Science Foundation of China (61205014, 61378060, 61378035, 61307067 and 11074105), the Doctoral foundation of Shandong Province (BS2012DX006). It is also supported by Dawn Program of Shanghai Education Commission (11SG44), Special-funded Program on National Scientific Instruments and Equipment Development (2012YQ170004).

References

1. E. X. Jin and X. Xu, *Appl. Phys. Lett.*, 2005, **86**, 111106.
2. K. A. Willets, *Phys. Chem. Chem. Phys.*, 2013, **15**, 5345–5354
3. P. Zijlstra, P. M. R. Paulo and M. Orrit, *Nat. Nanotechnol.*, 2012, **7**, 379–382.
4. S. Lal, S. Link and N. J. Halas, *Nat. Photonics*, 2007, **1**, 641–648.
5. Prodan, E., Radloff, C., Halas, N. J. & Nordlander, P., *Science*, 2003, **302**, 419–422.
6. Atwater, H. A. & Polman, A. *Nat. Mater.*, 2010, **9**, 205–213.
7. Altmewischer, E., van Exter, M. P. & Woerdman, J. P., *Nature*, 2002, **418**, 304–306.
8. Akimov, A. V., A. Mukherjee, C. L. Yu, D. E. Chang, A. S. Zibrov, P. R. Hemmer, H. Park & M. D. Lukin, *Nature*, 2007, **450**, 402–406.
9. Ebbesen, T. W., Genet, C. & Bozhevolnyi, S. I., *Phys. Today*, 2008, **61**, 44–50.
10. Engheta, N., *Science*, 2007, **317**, 1698–1702.
11. Liu, N., Lutz Langguth, Thomas Weiss, Jürgen Kästel, Michael Fleischhauer, Tilman Pfau & Harald Giessen, *Nat. Mater.*, 2009, **8**, 758–762.
12. Ergin, T., Stenger, N., Brenner, P., Pendry, J. B. & Wegener, M., *Science*, 2010, **328**, 337–339.
13. Bergin Gjonaj, Jochen Aulbach, Patrick M. Johnson, Allard P. Mosk, L. Kuipers and Ad Lagendijk, *Nat. photonics*, 2011, **5**, 360–363.
14. Zhuoxian Wang, Hong Wei, Deng Pan, and Hongxing Xu, *Laser Photonics Rev.*, 2014, 1–6, DOI 10.1002/lpor.201300215.
15. Jiannong Chen, *Plasmonics*, 2013, **8**(2), 931–936.
16. Ewold Verhagen, Albert Polman, and L. (Kobus) Kuipers, *Optics Express*, 2008, **16**(1), 45–57.
17. Shantha Vedantam, Hyojune Lee, Japeck Tang, Josh Conway, Matteo Staffaroni, and Eli Yablonovitch, *Nano Lett.*, 2009, **9**(10), 3447–3452.
18. Dang Yuan Lei, Alexandre Aubry, Stefan A Maier and John B Pendry, *New J. of Phys.*, 2010, **12**, 093030.
19. Thomas Søndergaard, Sergey I. Bozhevolnyi, Jonas Beermann, Sergey M. Novikov, Eloise Devaux, and Thomas W. Ebbesen, *Nano Lett.*, 2010, **10**, 291–295.
20. Zhaowei Liu, Jennifer M. Steele, Hyesog Lee, and Xiang Zhang, *Appl. Phys. Lett.*, 2006, **88**, 171108.
21. Chenglong Zhao, Yongmin Liu, Yanhui Zhao, Nicholas Fang & Tony Jun Huang, *Nat. Commun.*, 2013, DOI: 10.1038/ncomms3305.
22. Seung-Yeol Lee, Il-Min Lee, Junghyun Park, Sewoong Oh, Wooyoung Lee, *Phys. Rev. Lett.*, 2012, **108**, 213907.
23. Chenglong Zhao and Jiasen Zhang, *Opt. Lett.*, 2009, **34**(6), 2147–2149.
24. Chenglong Zhao and Jiasen Zhang, *Appl. Phys. Lett.*, 2011, **98**, 211108.

25. Chenglong Zhao and Jiasen Zhang, *ACS Nano*, 2010, **4**(11),6433-6438
26. Zheyu Fang, Qian Peng, Wentao Song, Fenghuan Hao, Jia Wang, Peter Nordlander, and Xing Zhu, *Nano. Lett.*, 2011, **11**, 893-987
27. Chenglong Zhao, Jiayuan Wang, Xiaofei Wu, and Jiasen Zhang, *Appl. Phys. Lett.*, 2009, **94**, 111105.
28. Qiwen Zhan, *Advances in Optics and Photonics*, 2009, **1**, 1–57.
29. R. Dorn, S. Quabis, and G. Leuchs, *Phys.Rev.Lett.*, 2003, **91**(23), 233901
30. Colin J. R. Sheppard and Amarjyoti Choudhury, *Appl. Opt.*, 2004, **43**(22), 4322-4327.
31. Gilad M. Lerman and Uriel Levy, *Opt. Express*, 2008, **16**(7), 4567-4581.
32. Han Lin and Min Gu, *Opt. Lett.*, 2011, **36**(13), 2471-2473.
33. Haifeng Wang, Luping Shi, Boris Lukyanchuk, Collin Sheppard, and Chong tow chong, *Nat. Photonics*, 2008, **2**, 501-505.
34. Jiannong Chen, Xiumin Gao, Linwei Zhu, Qinfeng Xu, Wangzi Ma, *Opt. Commun.*, 2014, **318**, 100-104.
35. Ayman F. Abouraddy and Kimani C. Toussaint, Jr, *Phys.Rev.Lett.*, 2006, **96**,153901.
36. Hong Kang, Baohua Jia, and Min Gu, *Opt. Express*, 2010, **18**(10), 10813-10821.
37. Hao Chen, Zhu Zheng, Bai-Fu Zhang, Jianping Ding, and Hui-Tian Wang, *Opt. Lett.*, 2010, **35**(16), 2825-2827.
38. Xiangping Li, Tzu-Hsiang Lan, Chung-Hao Tien & Min Gu, *Nat. Commun.*, 2012, **3**, DOI: 10.1038/ncomms2006.
39. Zhipeng Li, Timur Shegai, Gilad Haran, and Hongxing Xu, *ACS Nano*, 2009, **3**(3), 637-642.
40. Satoshi Kawata, Yasushi Inouye and prabhat Verma, *Nat. photonics*, 2009, **3**, 388-394.
41. Yuan Wang, Werayut Srituravanich, Cheng Sun, and Xiang Zhang, *Nano Lett.*, 2008, **8**(9), 3041-3045.
42. Jiao Lin, J. P. Balthasar Mueller, Qian Wang, Guanghui Yuan, 3 Nicholas Antoniou, Xiao-Cong Yuan, Federico Capasso, *Science*, 2013, **340**, 331-334.
43. Liang Pan, Yongshik Park, Yi Xiong, Erick Ulin-Avila, Yuan Wang, Li Zeng, Shaomin Xiong, Junsuk Rho, Cheng Sun, David B. Bogy & Xiang Zhang, *Scientific reports*, 2011, DOI: 10.1038/srep00175.
44. S. A. Maier, *Plamomics: Fundamentals and Applications*, Springer-Verlag, 2007, New York.
45. Takuo Tanemura, Krishna C. Balram, Dany-Sebastien Ly-Gagnon, Pierre Wahl, Justin S. White, Mark L. Brongersma, and David A. B. Miller, *Nano Lett.*, 2011, **11**, 2693-2698.